Diagnostic Performance of a Receptor-Binding Radiopharmacokinetic Model

David R. Vera, Robert C. Stadalnik, Charles E. Metz and Neville R. Pimstone
Division of Nuclear Medicine, Department of Radiology, and Division of Gastroenterology, Department of Internal Medicine, University of California, Davis; and Department of Radiology, University of Chicago, Chicago, Illinois

The aim of this study was to determine which measurement obtained from a radiopharmacokinetic model of a receptor-binding radiotracer provides the highest diagnostic performance for the detection of diffuse hepatocellular disease. **Methods:** Twenty-seven healthy subjects and 46 patients with diffuse hepatocellular disease were studied with the receptor-binding radiopharmaceutical, ^{99m}Tc-galactosyl-neoglycoalbumin. A radiopharmacokinetic model was used to produce estimates of receptor concentration $[R]_0$, the scaled forward-binding rate constant $\tilde{k}_b$, hepatic plasma volume, V_h, extrahepatic plasma volume, V_e and hepatic plasma flow, F. Receiver operating characteristic analysis of each model estimate was conducted. **Results:** Receptor concentration $[R]_0$ and the metrics $[R]_0$/tbw and $\tilde{k}_b[R]_0[R]_0$/tbw provided the best discrimination between healthy and diseased liver. The forward-binding rate constant $\tilde{k}_b$ and the metrics F/V_e and V_h/tbw provided no discrimination. **Conclusion:** Based on simplicity and higher measurement precision, $[R]_0$ was selected as the most accurate index of hepatic function.

Key Words: receiver operating characteristics; technetium-99m-galactosyl-neoglycoalbumin; radiopharmacokinetic modeling; receptor-binding radiopharmaceuticals

J Nucl Med 1996; 37:160–164

When the biodistribution of a receptor-based diagnostic agent is analyzed by a pharmacokinetic model, the opportunity exists for in vivo measurement of the physiologic and biochemical parameters that govern tissue uptake. Technetium-99m-galactosyl-neoglycoalbumin (Tc-NGA) (*1*) is a radiopharmaceutical that binds to the asialoglycoprotein receptor (ASGP-R), which is unique to the hepatocyte. Kinetic analysis (*2*) of a subject's heart and liver time-activity data yields five independent measurements: receptor concentration, Tc-NGA-receptor affinity, hepatic plasma volume, extrahepatic plasma volume and hepatic plasma flow. Previous clinical studies revealed a high correlation between receptor concentration (*3,4*) and other standard measures of hepatic function. Additionally, receptor concentration was able to differentiate (*5–9*) between normal and various forms of liver disease.

The purpose of the present study was to determine which measurement obtained from the kinetic analysis of Tc-NGA functional imaging provides the highest diagnostic performance for the detection of diffuse hepatocellular disease. To achieve this aim, we used receiver operating characteristic (ROC) analysis (*10*) of each measurement and various combinations and scalings.

Received Nov. 7, 1994; revision accepted May 16, 1995.
For correspondence or reprints contact: David R. Vera, PhD, Nuclear Medicine, University of California, Davis, Medical Center, Research I, Rm. 1001, 4815 Second Ave., Sacramento, CA 95817.

METHODS

Subjects

This study included 27 healthy volunteers, designated D^- subjects, and 46 patients, D^+ subjects, selected from the Hepatology Service at the University of California, Davis, Medical Center between July 1985 and October 1993. The study protocol was approved by the University of California, Davis, Human Subjects Review Committee and written informed consent was obtained from all subjects. Criteria for D^- subjects were the following: (a) no history of liver disease, (b) no known congenital forms of hepatic disease, (c) normal liver function as assessed by standard SMA-20, (d) no history of a medical condition likely to affect hepatic function, (e) no illnesses within 2 wk of the study, (f) no ingestion of drugs known to effect liver function. Criteria for D^+ subjects, based on hepatic biopsy, included all forms of post-necrotic cirrhosis and hepatitis. Subjects with known focal hepatic tumors and patients with primary biliary cirrhosis or primary sclerosing cholangitis were excluded. Pregnant and lactating females were excluded from the study. The 27 healthy volunteers and the 46 patients are the same subjects of a previous report (*9*), which utilized the same kinetic analysis software as this study.

Technetium-99m-NGA Functional Imaging

Synthesis (*11*), imaging (*1,9*) and kinetic analysis (*12*) were performed as previously described. Briefly, Tc-NGA functional imaging consists of a 30-min dynamic study during which 120 128 × 128 images of the heart and liver (anterior view) are acquired onto a standard nuclear medicine computer. The amount of Tc-NGA (18.5×10^{-10} mole NGA/kg) injected is based on the subject's total body weight. During the period from 3 to 5 min postinjection, up to four intravenous blood samples are withdrawn and used to calculate the fraction of injected dose per liter of plasma at 3 min postinjection. Time-activity curves for liver and heart are then generated by standard nuclear medicine software. This information was submitted with the subject's height, weight and sex to an automated program (NGAFIT version 6.1) to produce measurements (see Table 1) for the subject's receptor concentration $[R]_0$, forward-binding rate constant, $\tilde{k}_b$, hepatic plasma volume, V_h, extrahepatic plasma volume, V_e, and hepatic plasma flow, F. Two criteria were set as quality control (*9*) for the kinetic analysis. Estimates were deemed unacceptable if at least one blood sample was not obtained within the 3–5-min period postinjection or the total reduced chi square exceeded a predetermined level depending upon the receptor concentration estimate. Curve-fits that did not pass the above criteria were excluded from this study. A [^{14}C]aminopyrine breath test (ABT) (*13*) was conducted immediately after each Tc-NGA functional imaging study. If a subject was imaged multiple times, only the earliest study to pass the analysis criteria was included in the ROC analysis.

ROC Analysis

Receiver operating characteristic analysis (*10*) was conducted for each of the following metrics: $[R]_0$, $[R]_0$/tbw, R_0, R_0/tbw, $\tilde{k}_b$,

TABLE 1
Measurements from Kinetic Analysis of a Tc-NGA Functional Imaging Study

Symbol	Measurement	Units
$[R]_0$	Receptor concentration*	M
k_b	Forward-Binding rate constant	$M^{-1}min^{-1}$
V_h	Hepatic plasma volume	Liter
V_e	Extrahepatic plasma volume	Liter
F	Hepatic plasma volume	Liter/min

* Total receptor per volume of hepatic plasma.

$\tilde{k}_b[R]_0$, $\tilde{k}_b[R]_0[R]_0$/tbw, V_h/tbw, F/V_e, tbw and ABT. The metric $\tilde{k}_b$ is the scaled forward-binding rate constant calculated by:

$$\tilde{k}_b = k_b * 30/\rho_{gal}, \qquad \text{Eq. 1}$$

where ρ_{gal} is the carbohydrate density of the ^{99m}Tc-galactosyl-neoglycoalbumin. Pairs of metrics were submitted to the program CLABROC, which is a version of the program CORROC (*14*) that has been modified to analyze continuously distributed test results (*15*). CLABROC: (a) generated a ROC curve for each metric by selecting ten criteria points, (b) fit a binormal curve to each ROC, (c) calculated the area under each binormal curve, A_z^x and A_z^y, (d) calculated the standard deviations of each area, $SD(A_z^x)$ and $SD(A_z^y)$, and their correlation $r(A_z^x, A_z^y)$, and (e) determined the P value for the difference between paired areas, $A_z^x - A_z^y$. Lastly, the 95% confidence interval [LB, UB] (*16*) for the differences in A_z^x and A_z^y were calculated with the following equations:

$$LB = A_z^x - A_z^y - 1.96\ s.d.(\Delta A_z) \qquad \text{Eq. 2A}$$

$$UB = A_z^x - A_z^y + 1.96\ s.d.(\Delta A_z), \qquad \text{Eq. 2B}$$

where $s.d.(\Delta A_z)$ is the estimated standard deviation of the difference in A_z which was given by

$$s.d.(\Delta A_z) = \sqrt{[s.d.(A_z^x)]^2 + [s.d.(A_z^y)]^2 - 2s.d.(A_z^x)s.d.(A_z^y)r(A_z^x, A_z^y)}. \qquad \text{Eq. 3}$$

RESULTS

The metrics $\tilde{k}_b[R]_0[R]_0$/tbw, $[R]_0$/tbw, and receptor concentration $[R]_0$ provided the best diagnostic performance. Table 2 lists each metric, the measurement units and A_z the area (with standard error) under the binormal fit to the ROC data. The ROC data for each metric and with binormal fits are displayed in Figure 1. The ABT produced an ROC curve (Fig. 1A) with an A_z of 0.939 ± 0.030. The tbw yielded a nearly diagonal ROC curve (Fig. 1E) with an A_z of 0.640 ± 0.064. Metrics F/V_e and V_h/tbw (Figs. 1D, E), and the scaled forward-binding rate constant $\tilde{k}_b$ (Fig. 1D) also exhibited poor diagnostic performance: A_z equaled 0.643 ± 0.066, 0.520 ± 0.068 and 0.565 ± 0.067, respectively. Table 3 is a matrix which pairs the metrics for a statistical comparison of the A_z index. Listed is the probability value that the observed differences in the areas beneath each curve are due solely to chance. For example, Table 3 indicates a 0.8% probability that the observed difference between the A_z of the $\tilde{k}_b[R]_0[R]_0$/tbw ROC curve (Fig. 1B) and the A_z of the R_0 ROC curve (Fig. 1C) was due to chance alone.

DISCUSSION

Our selection of which metrics to include in this study was based on the expectation that intensive variables would provide the highest diagnostic performance. Intensive variables are independent of size (*17*). For example, we did not test V_e, an extensive variable, which is directly proportional to the subject's size. The desirability of intensive variables was the rationale for scaling by the subject's tbw. This normalizes the metrics $\tilde{k}_b[R]_0[R]_0$/tbw, R_0/tbw, and V_h/tbw to body weight. Model parameters k_b and $[R]_0$ are also intensive. As the forward-binding rate constant, k_b, governs the rate of receptor binding per receptor concentration, its magnitude is independent of receptor amount, the reaction volume, or the subject's size. Receptor concentration represents the total amount of hepatic receptor divided by the subject's hepatic plasma volume

$$[R]_0 = R_0/V_h. \qquad \text{Eq. 4}$$

It is therefore independent of the subject's weight.

The metric $\tilde{k}_b[R]_0[R]_0$/tbw represents the maximum transport binding capacity of the receptor per kilogram of body weight. It is similar to V_{max} (*18*) and R_{max} (*19,20*) indices of indocyanine green uptake. Based on the bimolecular reaction

$$[L] + [R] \underset{k_{-b}}{\overset{k_b}{\rightleftarrows}} [C], \qquad \text{Reaction I}$$

where [C], [R] and [L] are the concentrations of the ligand-receptor complex, free receptor and ligand at time t and k_{-b} is the reverse-binding rate constant. It is derived using the definition of the forward flux for the ligand-receptor complex

$$\frac{d[C]}{dt} = k_b[R][L] - k_{-b}[C]. \qquad \text{Eq. 5}$$

Because Tc-NGA-AGSP-R binding is operationally irreversible (*21*), reaction I simplifies to

$$[L] + [R] \xrightarrow{k_b} [C] \qquad \text{Reaction II}$$

and Equation 3 reduces to

$$\frac{d[C]}{dt} = k_b[R][L]. \qquad \text{Eq. 6}$$

The maximum value of d[C]/dt is attained when the receptor and ligand concentrations equal the maximum concentration of free receptor which occurs immediately before injection of Tc-NGA. Therefore, [R] and [L] are set equal to $[R]_0$ and the maximum transport capacity R_{max} becomes

TABLE 2
ROC Analysis

Metric	Units	A_z^*
$\tilde{k}_b[R]_0[R]_0$/tbw	M min^{-1}/kg	0.985 ± 0.011
$[R]_0$/tbw	M/kg	0.974 ± 0.018
$[R]_0$	M	0.965 ± 0.020
$\tilde{k}_b[R]_0$	min^{-1}	0.941 ± 0.026
ABT	%/hr	0.939 ± 0.030
R_0/tbw	mole/kg	0.933 ± 0.029
R_0	mole	0.875 ± 0.042
F/V_e	liter/min	0.643 ± 0.066
tbw	kg	0.640 ± 0.064
$\tilde{k}_b^{\dagger}$	$M^{-1}min^{-1}$	0.565 ± 0.067
V_h/tbw	liter/kg	0.520 ± 0.068

*Area under the binormal fit to the ROC data ± 1 s.e.
†Scaled forward-binding rate constant = $\tilde{k}_b * 30/\rho_{gal}$.

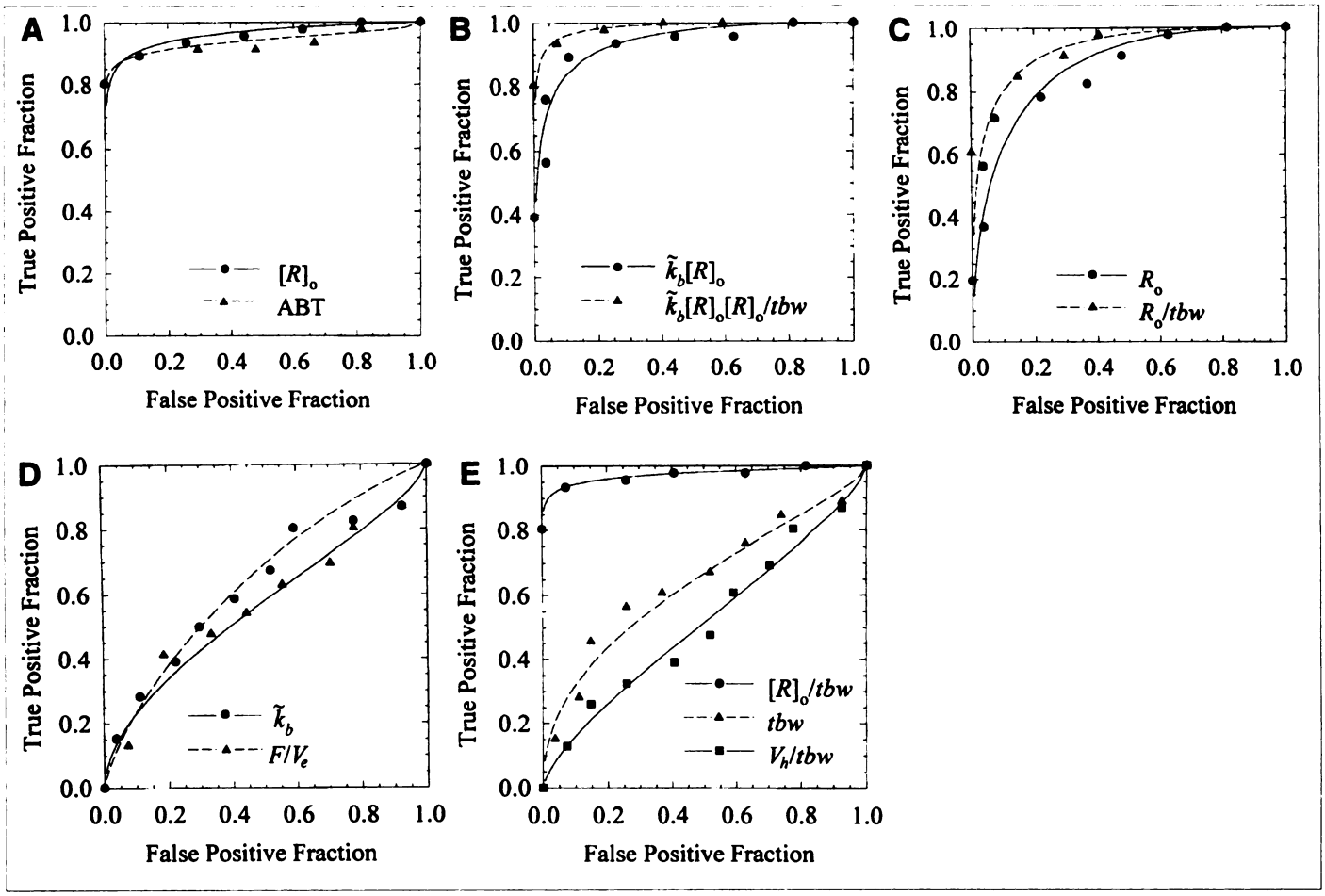

FIGURE 1. ROC analysis (symbols) and binormal curve-fits (lines) of: (A) receptor concentration $[R]_0$ (●) and the ABT (▲), (B) first-order rate constant $\tilde{k}_b[R]_0$ (●) and the receptor transport maximum $\tilde{k}_b[R]_0[R]_0/tbw$ (▲), (C) receptor amount R_0 (●) and R_0/tbw (▲), (D) forward-binding rate constant $\tilde{k}_b$ (●) and F/V_e (▲) and (E) $[R]_0/tbw$ (●), tbw (▲) and V_h/tbw (■).

$$R_{max} = k_b[R]_0[R]_0. \quad \text{Eq. 7}$$

After normalizing k_b to a carbohydrate density of 30 by Equation 1 and scaling by tbw, the scaled transport maximum $\tilde{R}_{max}$ for TcNGA is defined as

$$\tilde{R}_{max} = \tilde{k}_b[R]_0[R]_0/tbw. \quad \text{Eq. 8}$$

Metric F/V_e is an intensive variable and provides an index of hepatic perfusion independent of the subject's size. We selected F/V_e over F/tbw because the former parameter governs the delivery of drugs and nutrients to the liver. The metric V_h/tbw was selected as an index of hepatic plasma volume. We also selected R_0, the total hepatic receptor quantity, for ROC analysis. Our intention was to compare its diagnostic performance with the scaled metric R_0/tbw. If intensive variables are inherently more diagnostic than extensive variables, the area under the R_0/tbw ROC curve would exceed the A_z of the R_0

TABLE 3
Statistical Significance of A_z

	P value*									
Metric	$\tilde{k}_b[R]_0[R]_0/tbw$	$[R]_0/tbw$	$[R]_0$	$\tilde{k}_b[R]_0$	ABT	R_0/tbw	R_0	F/V_e	tbw	$\tilde{k}_b$
$[R]_0/tbw$	0.414									
$[R]_0$	0.188	0.406								
$\tilde{k}_b[R]_0$	0.070	0.221	0.342							
ABT	0.131	0.234	0.505	0.991						
R_0/tbw	0.065	0.143	0.282	0.828	0.909					
R_0	0.008	0.024	<0.001	0.108	0.183	0.025				
F/V_e	<0.001	<0.001	<0.001	<0.001	<0.001	<0.001	<0.001			
tbw	<0.001	<0.001	<0.001	<0.001	<0.001	<0.001	<0.001	0.989		
$\tilde{k}_b$	<0.001	<0.001	<0.001	<0.001	<0.001	<0.001	<0.001	0.342	0.426	
V_h/tbw	<0.001	<0.001	<0.001	<0.001	<0.001	<0.001	<0.001	0.263	0.200	0.374

*Two-tailed t-test.
tbw = total body weight.

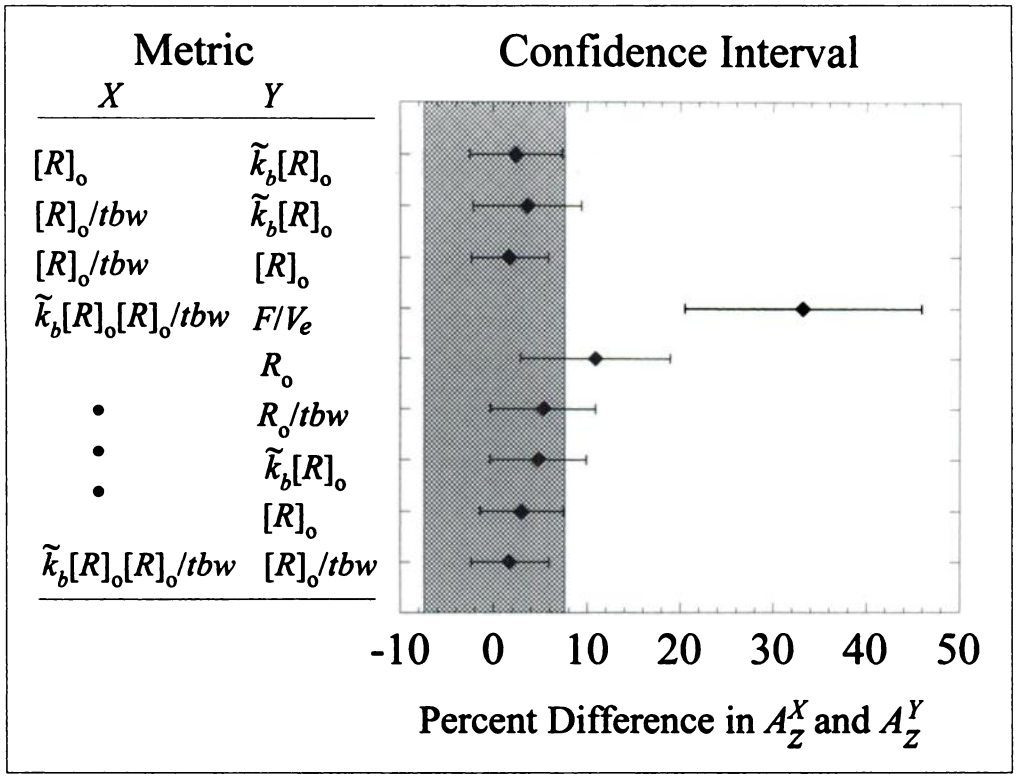

FIGURE 2. Clinical significance was determined by 95% confidence intervals of the differences in A_z. The difference in diagnostic performance of two metrics was deemed not clinically significant when the entire confidence interval is within the range defined by −7.5 through 7.5% difference in A_z (shaded area). Based on this criteria, we judged the diagnostic performance of metrics $\tilde{k}_b[R]_o[R]_o$/tbw, $[R]_o$/tbw and $[R]_o$ to be clinically equivalent. The vertical ellipsis (· · ·) signifies that the last five entries of the X metric are $\tilde{k}_b[R]_o[R]_o$/tbw.

metric. As illustrated in Figure 1C, R_0/tbw displayed higher diagnostic performance than R_0.

Our selection of $\tilde{k}_b[R]_0$ was based on an inherent kinetic property. This metric is termed the pseudo first-order, rate-binding constant and governs the rate of receptor binding. Many receptor-binding radiopharmaceuticals (*1*) cannot be used under the imaging conditions that permit kinetic analysis of k_b and $[R]_0$ as independent measurements. Therefore, these imaging studies produce $k_b[R]_0$ as a single value. We formed $\tilde{k}_b[R]_0$ by multiplication of the independent estimates of k_b and $[R]_0$ produced by the Tc-NGA kinetic analysis. This ability to independently estimate the forward-binding rate constant and receptor concentration with a single injection is unique to Tc-NGA functional imaging.

Lastly, we selected a metric tbw, which is not diagnostic for diffuse hepatocellular disease, and a metric that is a well-established index of hepatic function, the ABT. The metric from the ABT is the percent of administered ^{14}C exhaled per hour at 2 hr postadministration. This rate is governed by hepatic microsome enzymatic activity and is therefore an index of functional hepatic mass. As a result, the ABT and the receptor-based metrics, $\tilde{k}_b[R]_0[R]_0$/tbw, $[R]_0$/tbw, $[R]_0$, $\tilde{k}_b[R]_0$, R_0, R_0/tbw and R_0 of Tc-NGA functional imaging yield equivalent information.

Four of the Tc-NGA metrics, $\tilde{k}_b[R]_0[R]_0$/tbw, $[R]_0$/tbw, $[R]_0$, yielded larger areas under their ROC curves (Figs. 1A–C) than ABT. None of the areas, however, were statistically different ($p > 0.05$). All of these metrics produced statistically different ($p < 0.001$) areas than tbw, which, as anticipated, was of no diagnostic value ($A_z = 0.640 \pm 0.064$). Two Tc-NGA metrics, $\tilde{k}_b$ and V_h/tbw, performed worse than tbw, yielding near diagonal ROC curves. Consequently, the forward-binding rate constant k_b does not yield any diagnostic information. This, however, does not provide a sound rationale for the elimination of this parameter from the curve-fitting procedure by holding it constant during the estimation of $[R]_0$. It also does not provide a reason to numerically combine k_b with $[R]_0$ and estimate the pseudo first-order rate constant $k_b[R]_0$. The attraction to elimination k_b from the curve-fitting procedure would be faster execution of the curve fit and higher precision of $[R]_0$ estimates (*22*). The danger in not estimating k_b and $[R]_0$ simultaneously, which assumes an a priori knowledge of k_b, is the possible introduction of bias to $[R]_0$ if the assumed k_b is wrong.

Failure to demonstrate a statistically significant difference among the four metrics with the largest areas does not prove that no real difference exists. A conclusion, that a difference in diagnostic performance does not exist, is based on an estimated range of the true difference and the minimum clinically acceptable difference in detectability (ΔA_z). The 95% confidence interval (*16*) provides the estimate of this range. Figure 2 displays the 95% confidence intervals of the A_z differences of various metric pairs. The vertical ellipsis (· · ·) signifies that the last five entries of the X metric are $\tilde{k}_b[R]_0[R]_0$/tbw. The upper and lower vertical boundaries of the shaded area represent a minimum clinically acceptable difference of 7.5%. The difference in diagnostic performance of two metrics was deemed not clinically significant, when the entire confidence interval was within the range defined by the upper and lower boundaries (shaded area). Based on this, we judged the diagnostic performance of the following metrics to be clinically equivalent: $[R]_0$, $\tilde{k}_b[R]_0$; $[R]_0$/tbw, $[R]_0$; $\tilde{k}_b[R]_0[R]_0$/tbw, $[R]_0$; and $\tilde{k}_b[R]_0[R]_0$/tbw, $[R]_0$/tbw. The clinical significance between pairs $[R]_0$/tbw, $\tilde{k}_b[R]_0$; $\tilde{k}_b[R]_0[R]_0$/tbw, R_0; $\tilde{k}_b[R]_0[R]_0$/tbw, R_0/tbw; and $\tilde{k}_b[R]_0[R]_0$/tbw, $k_b[R]_0$ were deemed inconclusive. As an example of a clinically significant difference in diagnostic performance, we included the metric pair $\tilde{k}_b[R]_0[R]_0$/tbw, F/V_e. The lower bound

of the confidence interval did not include 7.5%, the upper boundary of the shaded area.

Because metrics $\tilde{k}_b[R]_0[R]_0/tbw$, $[R]_0/tbw$ and $[R]_0$ displayed equivalent diagnostic performance, we are left with a choice. Among these highest performers, we consider $[R]_0$ as the best choice. Our reasoning is based on simplicity and precision. Simplicity intuitively argues against a metric that includes the patient's body weight. It is an additional measurement which must be carefully obtained. Likewise, selecting a metric based on the criterion of high precision eliminates those composed of multiple model parameters. This is due to error propagation. For example, the coefficient of variation, $CV(\tilde{R}_{max})$, of $\tilde{k}_b[R]_0[R]_0/tbw$ equals

$$CV(\tilde{R}_{max}) = \sqrt{\left[\frac{SE(k_b)}{k_b}\right]^2 + \left[\frac{2SE([R]_0)}{[R]_0}\right]^2 + \frac{4Cov(k_b, [R]_0)}{k_b[R]_0}}, \quad \text{Eq. 9}$$

where $SE(k_b)$, $SE([R]_0)$, $Cov(k_b, [R]_0)$ are the standard errors of k_b and $[R]_0$ and the covariance of k_b with $[R]_0$. Typically, relative uncertainties in k_b and $[R]_0$ in healthy subjects are 30% and 10%, respectively (*23*). Due to error propagation from multiplication of $k_b[R]_0[R]_0$, the relative uncertainty of $\tilde{k}_b[R]_0[R]_0/tbw$ increases to approximately 45%. Consequently, this metric will have less precision than $[R]_0$. High precision will be most important when Tc-NGA functional liver imaging is used to follow the clinical course of an individual patient. Based on confidence interval analysis, the use of $[R]_0$ as the test criterion instead of $\tilde{k}_b[R]_0[R]_0/tbw$ could potentially result in a loss of 0.075 in A_z. At 90% specificity, this translates into a potential drop in sensitivity from 95% to 85%. This approximation is based on a 7.0% ΔA_z (Table 1) between $\tilde{k}_b[R]_0$ and R_0, and the sensitivity predicted by their ROC curves at 90% specificity (Figs. 1B, C). We consider the fourfold higher precision of $[R]_0$ to justify the decrease in sensitivity, the magnitude of which has a 5% probability of reaching 17%.

CONCLUSION

Receptor concentration $[R]_0$ exhibited the best balance between simplicity, precision and diagnostic performance. Therefore, this work confirms an early hypothesis (*24*) that a measurement of scaled functional hepatic mass, the amount of receptor per volume of hepatic plasma $[R]_0$, will provide the highest diagnostic power.

ACKNOWLEDGMENTS

The authors thank Dusan P. Hutak for his excellent technical assistance and Dr. William C. Eckelman for his helpful discussions. This work was supported by U.S. Public Health Service grants RO1 AM34768 and RO1 AM34706.

REFERENCES

1. Stadalnik RC, Kudo M, Eckelman WC, Vera DR. In vivo functional imaging using receptor-binding radiopharmaceuticals: technetium-99m-galactosyl-neoglycoalbumin as a model. *Invest Radiol* 1993;28:64–70.
2. Vera DR, Stadalnik RC, Trudeau WL, Scheibe PO. Measurement of receptor concentration and forward binding rate constant via radiopharmacokinetic model of [^{99m}Tc]galactosyl-neoglycoalbumin. *J Nucl Med* 1991;31:1169–1176.
3. Stadalnik RC, Vera DR, Woodle ES, et al. Technetium-99m-NGA functional hepatic imaging: preliminary clinical experience. *J Nucl Med* 1985;26:1233–1242.
4. Kudo M, Vera DR, Stadalnik RC, Trudeau WL, Ikekubo K, Kudo A. In vivo estimates of hepatic binding protein concentration: correlation with classical indicators of hepatic functional reserve. *Am J Gastroenterol* 1990;85:1142–1148.
5. Virgolini I, Müller C, Klepetko W, et al. Decreased hepatic function in patients with hepatoma or liver metastasis monitored by a hepatocyte-specific galactosylated radioligand. *Br J Cancer* 1990;61:937–941.
6. Virgolini I, Müller C, Höbart J, et al. Liver function in acute viral hepatitis as determined by a hepatocyte-specific ligand: ^{99m}Tc-galactosyl-neoglycoalbumin. *Hepatology* 1992;15:593–598.
7. Kudo M, Todo A, Ikekubo K, Yamamoto K, Vera DR, Stadalnik RC. Quantitative assessment of hepatocellular function via in vivo radioreceptor imaging: technetium-99m-galactosyl human serum albumin (Tc-GSA). *Hepatology* 1993;17:814–819.
8. Virgolini I, Kornek G, Höbart J, et al. Scintigraphic evaluation of functional hepatic mass in patients with advanced breast cancer. *Br J Cancer* 1993;68:549–554.
9. Pimstone NR, Stadalnik RC, Vera DR, Hutak DP, Trudeau WL. Evaluation of hepatocellular function by way of receptor-mediated uptake of a technetium-99m-labeled asialoglycoprotein analogue. *Hepatology* 1994;20:917–923.
10. Metz CE. ROC Methodology in radiologic imaging. *Invest Radiol* 1986;21:720–733.
11. Vera DR, Stadalnik RC, Krohn KA. Technetium-99m-galactosyl-neoglycoalbumin: preparation and preclinical studies. *J Nucl Med* 1985;26:1157–1167.
12. Vera DR, Scheibe PO, Krohn KA, Trudeau WL, Stadalnik RC. Goodness-of-fit and local identifiability of a receptor-binding radiopharmacokinetic system. *IEEE Trans Biomed Eng* 1992;BME-39:356–367.
13. Galizzi J, Long RG, Billing BH, Sherlock S. Assessment of the [^{14}C]aminopyrine breath test in liver disease. *Gut* 1978;19:40–45.
14. Metz CE, Wang P-L, Kronman HB. A new approach for testing the significance of differences between ROC curves measured from correlated data. In: Deconinck F, ed. *Information processing in medical imaging*. The Hague: Nijhoff; 1984:432–445.
15. Metz CE, Shen J-H, Herman BA. New methods for estimating a binormal ROC curve from continuously-distributed test results. *1990 Joint Statistical Meetings of the American Statistical Society and the Biometric Society*. Anaheim, CA, 1990.
16. Metz CE. Quantification of failure to demonstrate statistical significance: the usefulness of confidence intervals. *Invest Radiol* 1993;28:59–63.
17. Moore WJ. *Physical chemistry*, 4th ed. Englewood Cliffs, NJ: Prentice-Hall, 1972.
18. Paumgartner G, Probst P, Kraines R, Leevy CM. Kinetics of indocyanine green removal from the blood. *Ann NY Acad Sci* 1970;170:134–147.
19. Moody FG, Rikkers LF, Aldrete JS. Estimation of the functional reserve of human liver. *Ann Surg* 1974;180:592–598.
20. Kudo M, Vera DR, Stadalnik RC, et al. Measurement of functioning hepatocyte mass via [^{99m}Tc]galactosyl-neoglycoalbumin. *Dig Dis Sci* 1993;38:2183–2188.
21. Vera DR, Krohn KA, Stadalnik RC, Scheibe PO. Technetium-99m-galactosyl-neoglycoalbumin: in vitro characterization of receptor-mediated binding. *J Nucl Med* 1984;25:779–787.
22. Vera DR, Krohn KA, Scheibe PO, Stadalnik RC. Identifiability analysis of an in vivo receptor-binding radiopharmacokinetic system. *IEEE Trans Biomed Eng* 1985;BME-32:312–322.
23. Vera DR, Scheibe PO, Banin Y, Stadalnik RC. Local identifiability of a receptor-binding radiopharmacokinetic system having parameters of known uncertainty. *IEEE Trans Biomed Eng* 1994;BME-41:891–897.
24. Stadalnik RC, Vera DR, Krohn KA. Receptor-binding radiopharmaceuticals: Experimental and clinical aspects. In: Freeman LM, Weissman HS, eds. *Nuclear medicine annual 1986*. New York: Raven Press; 1986:105–139.